6

Nanotechnology-Based Biosensors in Drug Delivery

Guigen Zhang

Introduction

Traditional drug delivery vehicles are passive devices functioning mainly through a diffusion process in which the release of drugs is controlled either by the rate of diffusion through the pores of the drug carriers or by the rate of degradation of the carrier matrices. This passive process lacks the mechanism for a constant and on-demand means to administer drug delivery as needed. This has led to inability to deliver therapeutic moieties that can selectively reach the desired targets with marginal or no collateral damage to the normal organs and tissues (Ferrari, 2005).

Over the years, progresses have been made to improve the situation, specifically in ways to guide the accumulation of the drug delivery vehicles to desired sites and control the release mechanism (Barratt et al., 2002). For example, as a first generation of drug delivery systems, micro-capsules are often used for controlled release of proteins, peptides, or drugs within the body. Although they are capable of releasing the active substances at a somewhat desirable rate, they lack the ability to locate the specific site for action. The second-generation systems use environmental-sensitive (e.g., pH, temperature, or pressure sensitive) micro- or nanocapsules or magnetic spheres as delivery vehicles. With these added features, these drug delivery systems will release their payload upon receiving a specific signal such as a preset pH or temperature (Sawant et al., 2006). The third-generation systems are based on drug-carrying micro- or nano-shells or matrices that are functionalized with specific bioreceptors for specific target recognition. This feature adds the ability for these systems to self-recognize their target sites. Future drug delivery vehicles should be autonomous systems with both the diagnostic and therapeutic functionalities so that they will be able to constantly monitor the biological and physiological conditions, process the information, and administer the drug at a desired location, rate, and amount.

As drug delivery devices, these autonomous systems should ideally be small enough to be placed at, or be able to travel through, any desired location in the body. This has become increasingly feasible as the field of nanotechnology advances. Nanotechnology, by definition, deals with the observation, measurement, manipulation and fabrication of systems and

M.M. de Villiers et al. (eds.), *Nanotechnology in Drug Delivery*, DOI: 10.1007/978-0-387-77667-5_6,

constructs having dimensions themselves, or of their essential components, in the 1 nm–100 nm range at least in one dimension. Besides being small, nanotechnology offers materials and structures with unprecedented mechanical, physical, chemical, and biological properties and characteristics. In a sense, nanotechnology takes advantage of the analytical techniques and methodologies of multiple disciplines including mathematics, physics, chemistry, mechanical and electrical engineering, materials science, and molecular biology for the creation of new materials, constructs, devices, and systems.

For realizing such small autonomous systems for drug delivery, reliable nanotechnology-based biosensors are needed in the first place. This chapter will focus on some of the basic attributes of nanotechnology-based biosensors. The advantages of nanotechnology-based biosensors and the uniqueness of various common sensitive elements along with different underlying transducers will be discussed. Following that, some developments in nanostructure-based electrochemical biosensors will be discussed in detail. Finally, some future prospect for the development of nanotechnology-based biosensors will be presented.

The Advantages of Nanotechnology-Based Biosensors

Going nano means not only the size of a matter will be reduced but also the matter can be manipulated on the molecular and atomic levels. As a result, it will bring many benefits. In the case of a nanoparticle or a quantum dot, for example, reducing the size will increase the surface activity and induce unique quantum effects (e.g., confinement of electrons or photons by controlling the densities of electron states or photon states). This in turn will lead to unprecedented electronic, optical, and magnetic properties of the nanoparticle and quantum dot. Furthermore, the ability to arrange and rearrange atoms and molecules at will in a material will help render novel physical and chemical properties for the material.

In the case of biosensing, at the component level going nano means that the capability to sense and detect the state of biological systems and living organisms will be radically transformed by the emerging ability to control the patterns of matter on the nanometer scale (Alivisatos, 2004). Such a radical transformation is expected to enable sensing at the single-molecular level and with parallel detection of multiple signals in living cells. At the systems level, going nano will help decrease the size of the active sensing element to the scale of the target species (to increase the sensitivity and decrease the lower detection limit), reduce the required volumes of the analyte reagent, and minimize the detection time. Reducing the size of biosensors can also result in tiny devices which maybe deployable to any desired location in the body.

Sensors for Biosensors

In today's definition, biosensors are analytical devices that combine a biological-sensitive element with a physical transducer to selectively and quantitatively detect the presence of specific compounds in a given

biological environment. The biological-sensitive element consists of biological receptors (as probes) made of molecular species such as antibodies, enzymes, or nucleic acids for binding the target analytes, and the physical transducer is for converting the biological recognition or binding event into an electrical or optical signal. Thus, from a material's viewpoint, today's biosensors consist of two major components: an organic part as the sensitive element and an inorganic part as the transducer element.

In the future, the approach to biosensing may be drastically different. It is not inconceivable that future biosensors could be made of completely organic assemblies with the capability to communicate with external analytic and monitoring devices via a wireless means either electrically or optically. Currently, biosensors can be categorized mainly into two groups: in vivo and ex vivo biosensors according to their functions. In vivo biosensors are devices residing inside the body, either for a short or a prolonged period of time, for monitoring the biological target species, while ex vivo biosensors are devices for analyzing biological analyte species outside the body.

Basic Requirements for a Biosensor

A biosensor is, first of all, a sensor. This means that it needs to meet the basic requirements for any sensor: being sensitive, responsive, and reliable over a long period of time. Here reliability can be considered as being functioning well without producing false negative and/or false positive responses. But unlike a conventional sensor, a biosensor is often exposed to an environment containing many biological species that are similar in structures and binding behavior. Thus, in additional to meeting the above basic requirements, a biosensor needs to be specific, that is, be responsive only to a specifically targeted analyte species. With such specificity, the usefulness and reliability of a biosensor can be assured. Furthermore, because of the harsh and complex biological environment a biosensor often encounters, the loss of activity in the sensitive element is a major cause for the compromise of the reliability of a biosensor. This loss is mainly due to either the degradation of the molecular probes or their encapsulation (often termed fouling) by other microorganisms or large molecular weight proteins (Ratner et al., 2004). Thus, for a biosensor, the molecular probes to be used need to have long-lasting activity and antifouling behavior.

Due to the difference in their operational environments, in vivo and ex vivo biosensors often face different requirements for their fabrication. An in vivo biosensor has to be constructed using materials that are biocompatible with the body because of its implantation nature. Furthermore, the whole implanted in vivo device should not be encapsulated by the fibrous tissues in the body.

Various Sensitive Elements

Biosensors can be classified according to the type of their sensitive element. Currently, five types of sensitive elements are mainly being used, namely antibodies, nucleotides, enzymes, cells, and synthetic molecules (Kubik et al.,

2005). Biosensors using antibodies as the sensitive element operate based on the binding of an antigen to a specific antibody. Such biosensors are often used in conditions where nonspecific interactions are minimized. Biosensors with nucleotides as the sensitive element are usually used to target the genetic materials such as DNA. Because they rely on the complimentary binding of paired single strands of DNA, this class of biosensors often provides good specificity in detection. The challenge for nucleotide-based biosensors, however, is that the number of target nucleotides is usually very small, thus posing a need for making sufficient copies of the target nucleotides before an actual detection can take place. Biosensors using enzymes as the sensitive element operate based on catalytically induced chemical reactions. The use of enzymes in this class of biosensors adds certain degree of complexity. For instance, while some enzymes require no additional compounds for activity, many enzymes require a cofactor (i.e., either inorganic ions or complex organic or metalloorganic molecules) for their activity. Moreover, the catalytic activity of enzymes is governed by the integrity of their native protein conformation. When enzymes are denatured or dissociated, their catalytic activity will be destroyed, which in turn will compromise the reliability of the biosensors. Because of this, this class of biosensors often exhibits a degrading sensing performance over time.

Cell-based biosensors are another important class of sensors gaining more and more attention lately. The use of whole cells as the sensitive element is very attractive because cells can provide highly selective and sensitive receptors, channels, and enzymes. The main advantages of cell-based biosensors are that cells have built-in natural selectivity to biologically active chemicals and that cells can react to analytes in a physiologically relevant mode (Bousse, 1996; Stenger et al., 2001). With a cell-based biosensor, measurements of transmembrane potential, impedance, and metabolic activity can be made. Challenges abound, however, for long-term operations of this class of biosensors because the viability of the cells must be maintained under various harsh operating conditions. To date, cells such as neurons (Borkholder et al., 1997), cardiac myocytes (Pancrazio et al., 1998), liver cells (Powers et al., 2002), and genetically engineered B cells (Rider et al., 2003) have been used as the sensitive elements. Besides these cells, microorganisms and bacterial cells have also been used as the sensitive elements in biosensors for the detection and monitoring of environmental pollutants (D'Souza, 2001) and evaluation of the effectiveness of drugs (Reining-Mack et al., 2002; Thielecke et al., 2001). Whole cell-based biosensors can offer tremendous benefits for screening drugs and studying the effects of biochemicals on multi-cellular organisms.

Synthetic molecule-based biosensors often use synthetic polymers such as aptamers as the sensitive element (Cai et al., 2006). Aptamers are synthetic nucleic acids that can be synthesized to couple (or fit) with amino acids, drugs, proteins, and other non-nucleic molecules. Because of that, this class of biosensors can provide high affinity to a wide array of targets with excellent specificity. Furthermore, these biosensors can maintain prolonged reliability due to the synthetic nature of the polymeric-sensitive element which will not denature over time.

To be functional, these sensitive elements need to be immobilized onto the surface of an underlying transducer. The duty of such an underlying

transducer is to convert a biological recognition, binding, or reaction event into an electrical or optical signal. Many different detection methods and techniques have been used for fulfilling such a duty as the underlying signal transducer.

Various Underlying Detection Methods

For the underlying detection methods, various physical and chemical techniques are used for converting the biological recognition or binding events into electrical or optical signals. These methods can be generally categorized into mechanical, optical, electromagnetic, electrical, thermal, magnetic and electrochemical methods. The details of the operational principles for the mechanical, optical and electromagnetic, electrical and electrochemical methods are discussed here.

Mechanical Detection

In general, a mechanical-based transducer relies on either mechanical deformations or mechanical waves (or acoustic waves) as its sensing mechanism. To implement such a detection method, a mechanical structure in the form of a cantilever beam, a double-clamped beam, or a disc is often used as the underlying transducer, with the surface of the transducer functionalized by immobilizing a layer of a sensitive element (e.g., antibodies or enzymes) on it for target binding. Before further miniaturization is realized, this type of mechanical detection is better suited for ex vivo applications.

In the case of a cantilever beam, a common mode of detection is through the measurement of cantilever defection caused by the surface stresses generated as a result of molecular binding. Its working principle relies on the induced differential surface stress produced when molecules bind to one side of the cantilever surface (Berger et al, 1997; Sepaniak et al., 2002; Cherian et al., 2003). Surface stress mainly arises from intermolecular forces such as electrostatic interaction or van der Waals. Once generated, the differential stress will cause the cantilever to deflect. According to the classical work by Stoney (1909), for a fixed set of cantilever geometric and material properties, its deflection is linearly proportional to the differential surface stress which is related to the amount of molecular binding. The cantilever deflection is often measured by two common techniques. The first one is via an optical means in which a laser beam is focused on the free end of the cantilever and the cantilever deflection is measured with a four-segment photo detector. The second technique is through an electrical means in which a resistive or capacitive circuitry is used to measure the cantilever deflection (Porter et al., 2003). This mode of mechanical detection has its advantages. For example, when a flexible nanometer-scale cantilever is used, this class of mechanical biosensors is capable of detecting mismatches in oligonucleotide hybridization without labeling (Carrion-Vazquez et al., 1999) and of performing protein recognition with extremely high sensitivity. Moreover, this method is compatible with many analyte species in gaseous or aqueous forms (Wu et al., 2001). There are limitations as well. If the molecular binding events are exothermic, the heat generated may compromise the detection because a

differential thermal stress will also lead to deflection in the cantilever (Mertens et al., 2003). Another issue is with the nonlinear and viscoelastic nature of the molecular structures which may render it invalid to use Stoney's equations in interpreting the relationship between the measured cantilever deflection and the amount of molecular binding (Zhang & Gilbert, 2004; Zhang, 2005).

In the cases of a double-clamped beam or a disc structure, a common mode of detection is through the changes in the acoustic characteristics such as the resonant frequency, attenuation, and phase of wave propagation. In this mode of detection, the mechanical structures operate like oscillators, and a molecular binding event serves as mass loading which often leads to either a shift in the resonant frequency, an increase in amplitude attenuation, or a delay in the phase of wave propagation. Its basic operating principle relies on the fact that any mechanical structure possesses a unique resonate frequency (the lowest eigen frequency of the structure) along with a certain amount of attenuation and phase of propagation. When molecular binding occurs at the active surface of such a mechanical structure, the mass of the structure and damping to the wave propagation will increase (Headrick et al., 2003). Under this circumstance, the structure will exhibit certain changes in its wave characteristics when it is perturbed by an external acoustic wave. To increase the detection sensitivity, the mechanical structure (a beam or disc) should possess a high-quality factor (Davis et al., 2002). In general, the quality factor decreases when the size and damping of the mechanical structure increase. Bulk acoustic waves are more susceptible to liquid-damping-induced attenuation than surface acoustic waves; thus detections based on bulk acoustic waves (in the cases of a double-clamped beam or a quartz crystal microbalance) are preferably used in a dry environment and detections based on surface acoustic waves are often used in a liquid environment. A detailed discussion of the applications of bulk and surface acoustic wave devices can be found in a review by Rao and Zhang (2006). By detecting the frequency shift, the attenuation drop, and the phase shift, the amount of bound analyte can be determined. The advantage of this mode of detection is that a single frequency sweep can provide a quick measurement of the mass of the bound molecules at a resolution down to picogram level (Thundat et al., 1995). The challenge for this type of mechanical detection, however, lies in the difficulty in distinguishing the type and the uniformity of the bound species, thus rendering it less specific in biological sensing.

Optical and Electromagnetic Detection

Optical detection is one of the widely used mechanisms for biosensing because this method can be incorporated into many different types of spectroscopic techniques, including luminescence, absorption, polarization, and fluorescence (Wickline & Lanza, 2003). With this detection method, different spectrochemical properties such as amplitude, energy, polarization, decay time, and phase of a target analyte can be measured. These spectroscopic properties can be correlated to the concentration of the analyte of interest.

Of the many optical techniques, fluorescence-based detection is probably the most used method. In this method, fluorescent markers that emit

light at specific wavelengths are used as detecting labels for the target analytes, and measurements of fluorescent intensity are made for the presence of the targets or the binding of targets to the probes. Many micro-array gene chips use this technique for the detection of hybridization. Furthermore, fluorescence-based detection methods have been used to systematically analyze protein–protein and protein–DNA interactions. This technique has been proved capable of single molecule detection (Vo-Dinh & Cullum, 2000; Nie & Zare, 1997; Moerner & Orrit, 1999).

The sensing principle based on the evanescent wave is another common mode of optical detection. In this method, an optical waveguide is used to confine the light traveling through the waveguide by total internal reflection. With a majority part of the light confined inside the waveguide, a small part of it (i.e., the evanescent wave field) travels through a region that extends about several tens of nanometers into the surrounding medium. This evanescent wave can be used for sensing purposes. In a sensing application, the waveguide surface is functionalized with a biological-sensitive element, and the change in the optical properties of the evanescent wave is measured in response to the binding of the target and probe molecules. Evanescent wave-based sensors are very selective and sensitive for the detection of low levels of chemicals and biological species, and they are suited for the measurement of molecular interactions in situ and in real time (Liu & Tan, 1999). One of the most used evanescent wave biosensors is the surface plasmon resonance (SPR) sensor owing to its high sensitivity and simplicity. In a SPR sensor, the change in the refractive index of the evanescent wave, caused by the interaction between the target molecules and the sensitive probing molecules immobilized on the sensor surface in the evanescent field, is measured.

A well-known electromagnetic detection method is based on the theory of surface-enhanced Raman spectroscopy (SERS). Surface-enhanced Raman scattering is observed for molecules placed close to a rough metal surface featured with silver or gold nanostructures (e.g., nanoparticles or nanowires) because of surface plasmon resonance. This makes SERS a very sensitive detection technique. The working mechanism by which a SERS detection operates is still a debating issue. It is believed that it operates from a local electromagnetic field enhancement provided by an optically active nanoparticle. The electromagnetic effect alone, however, does not account for all that is observed through SERS. Molecular resonances, charge-transfer transitions, and other processes such as ballistic electrons transiently probing the region where the molecule resides and modulating electronic processes of the metal certainly contribute to the rich information that SERS measures (Moskovits, 2005). Nevertheless, ultrasensitive analytical strategies and bioassays based on SERS have been realized (Emery et al., 1998: Krug et al., 1999), in which an enhancement as large as 10^{14}, enough to allow routine detection of Raman from single molecules, is achieved.

Electrical Detection

Although it has not been as widely used as the mechanical or optical detection methods, electrical detection actually possesses some desirable features as an underlying transducer due to its ease of use, label-free

detection capability, portability, and miniaturization. Conductometric and potentiometric techniques are two common modes of electrical detection, and they mainly rely on the measurement of changes in conductance (or impedance) and potential in response to a biological binding event occurring at the electrode surfaces.

Conductometric sensors detect changes in the electrical resistance or impedance between two electrodes (Chen et al., 2003, 2004). In this case, the changes in resistance or impedance are due to either molecular interactions between nucleotides, proteins, and antigens and antibodies or excretion of metabolites near the electrode surfaces or in the surrounding media. This mode of detection is attractive because it does not require a specialized reference electrode as in the case of electrochemical detection. So far, this method has been used to detect a wide variety of chemical and biological target species, toxins, and nucleic acids, to measure the metabolic activity of microorganisms, and to monitor DNA hybridization (Sosnowski et al., 1997; Marrazza et al., 1999; Drummond et al., 2003). Currently, a practical challenge for a conductance base biosensing method is the understanding of the underlying mechanism for the changes in electrical properties of the electrode material caused by molecular adsorption and coupling.

Potentiometric sensors measure the potential changes between electrodes. The most common design of potentiometric sensors uses ion-sensitive field effect transistors or chemical field effect transistors (Bashir, 2004). A pH meter is such an example. Potentiometric sensors have been used to perform label-free detection of hybridization of DNA by measuring the field effect in silicon due to the intrinsic molecular charges on the DNA (Fritz et al., 2002). Recently, potentiometric sensors have been miniaturized to nanometer dimension through the use of silicon nanowires (Cui et al., 2001) and carbon nanotubes (Besteman et al., 2003) for enhanced sensitivity due to the increased surface to volume ratio for the electrodes.

Electrochemical Detection

Biosensors using an electrochemical method as the underlying transducer are often used to measure electrical responses resulted from the electrochemical reactions of the target redox species catalyzed by the enzymatic-sensitive element. These biosensors are usually configured in a three-electrode format: a working electrode, a counter electrode, and a reference electrode. The reference electrode needs to meet the special requirement of maintaining at a constant potential with respect to the electrolytic solution.

For biological detections, three modes of operations, namely amperometric, voltammetric, and impedimetric, are most commonly used. Amperometric biosensors measure the electrical current generated by the electron exchange between the electrodes and ionic species in response to electrode polarization at a constant potential. The measured steady-state limiting current (due to the encountered diffusion limit) is linearly proportional to the concentration of the electroactive analyte species. Voltammetric biosensors measure the current–potential relationships (i.e., voltammograms) induced by a redox process. The obtained peak currents and peak potentials (oxidation and reduction), or limiting currents in the

case of sigmoidal voltammograms for nanometer electrodes, are related to the transport phenomena and efficiency as well as the concentration of the redox species. Impedimetric biosensors measure the changes in the complex impedance of an electrochemical process upon cyclic excitations of the working electrode at a predetermined range of frequency. The measured results, often in Bode plots or Nyquist plots, are indicative of the electron transfer resistance which is related to the electrode/solution interfacial properties and the concentration of the analyte.

For the functionalization of these biosensors, enzymes are often used for catalytic-based sensing and other sensitive receptors (e.g., antibodies, nucleotides, cells, and proteins) are used for affinity-based sensing. In the case of a glucose sensor, the working electrode is usually functionalized with glucose oxidase for catalyzing glucose oxidation, and the current response is measured. Electrochemical-based biosensors have been used in the detection of glucose, lactose, urea, lactate, and DNA hybridization (Hintsche et al., 1991, 1995; Umek et al., 2001; Cia et al., 2002; Popovich & Thorp 2002; Zhu & Snyder, 2003).

Biosensors for Drug Delivery

Although future drug delivery devices may be autonomous systems with integrated capabilities of biosensing and drug delivery, the actual realization of such capabilities will rely on further advances in nanotechnology. Many progresses have been made in the development of lab-on-a-chip microscale devices (Bashir, 2004), and surely these devices will become more compact and more functional with higher sensitivity, specificity, and reliability in terms of sensing and with higher controllability in terms of drug delivery as the field of nanobiotechnology advances, but full-fledged autonomous systems of biosensors for drug delivery applications may still be years away. Currently, the development of biosensors for drug delivery takes a slightly different route. As discussed in the Introduction, drug delivery systems have been evolving from the totally passive drug-carrying vehicles of the first-generation systems, the environmental-sensitive drug-carrying vehicles of the second-generation system, to the target-specific and bioactive drug-carrying vehicles of the third-generation systems. Following this route, one can see that by adding sensitive components to the drug delivery systems, integrated capabilities of biosensing and drug delivery can be realized. Thus, it is conceivable that the next-generation drug delivery systems could be biologically sensitive drug-carrying vehicles incorporated with an underlying transducer (e.g., optical or image based) for signal detection and communication. This route may eventually converge with the lab-on-a-chip route, leading to an autonomous system with both the diagnostic and therapeutic functionalities.

But for now, one of the challenges in developing biosensitive drug delivery vehicles is to devise drug carriers that are biocompatible, resistive to biodegradation, resistive to host inflammatory and immunologic responses, and sensitive to specific targets, among other things. In addition, the drug carrier constructs should be highly effective in prolonged drug retention, especially for water-soluble drugs. Biological constructs such as liposomes are potentially good drug carrier materials due to their

abilities to protect drugs from degradation and to target the specific site for action (Knight, 1981). Because of their low encapsulation efficiency, rapid leakage of water-soluble drugs in the presence of blood elements, poor storage stability, and susceptibility to immunologic attacks, their application as drug carriers is severely hampered. To overcome this obstacle, a polymer coating that protects the liposomes from immunologic destruction and other degradation has been applied to form the so-called stealth-liposomes. In contrast, synthetic conjugated molecular assemblies and nanocapsules are more efficient drug carriers, and they have been used for many drugs including antibiotics, antiviral drugs, vitamins, proteins, peptides, enzymes, hormones, and oligonucleotides (Sun et al., 2006). Encapsulation is attractive because it can reduce systemic toxicity, protect vulnerable molecules from degradation in the digestive tract, and provide controlled release properties. Nanocapsules as drug carriers have been shown to protect insulin from degradation by digestive enzymes, to provide prolonged therapeutic effect, and to reduce drug-related immunologic responses (Aboubakar et al., 2000; Damage et al., 1997; Fernandez-Urrusuno et al., 1999).

For the nanocapsule-based biosensitive drug delivery systems, they should ideally be able to accumulate at specific sites of an organ or tissue, penetrate into target cells, and release the payload drug. The current systems rely on the immobilization of specific bioreceptors onto these drug carriers to perform site-specific targeting. To fulfill the cell-wall penetration function, it is necessary for these biosensitive drug carriers to have multiple active moieties for multiple functions including site-specific targeting and cell-wall penetration. These multiple moieties should be able to switch on and off upon certain environmental stimulations (e.g., pH, temperature, ion concentration, or partial pressure of oxygen and carbon dioxide).

Nanostructure-Based Electrochemical Biosensing

Electrochemical-based biosensing method is unique in many aspects including high sensitivity and specificity, low cost, ease of use, and ease of integration with micro-/nano-electronic and fluidic devices. To enhance the performances of such a sensing method, electrodes incorporated with arrays of nanostructures such as nanorods, nanowires, nanotubes, and nanopillars have been recently explored (Bharathi & Nogami, 2001; Koehne et al, 2004; Anandan et al, 2005, 2006). Because of the ultrasensitivity provided by these nanostructures having critical dimensions less than the lengths of the diffusion layer typically encountered on voltammetric time scales, investigation of electrochemical phenomena in fast-electron transfer reactions by steady-state experiments becomes possible (Arrigan, 2004). The use of these nanostructured electrodes in biosensors has extended electrochemical methodology into previously inaccessible domains of time, space, and medium. For example, electrodes incorporated with nanostructures are found to enhance significantly the electrochemical performances in DNA and glucose detections (Wang & Mustafa, 2004; Gasparac et al., 2004; Yemini et al., 2005; Anandan et al, 2006).

In an electrochemical biosensor, the dimension of its electrodes plays a significant role affecting the sensing performance. Electrodes with a smaller critical dimension can enable 3D radial nonlinear diffusion and provide steady-state voltammetric response. Because of the unique metal/solution interface in an electrochemical process, electrodes are often surrounded by an electrical double layer (EDL) structure. As the electrode size becomes equivalent to that of EDL (e.g., a fraction of a nanometer), the electrical field generated near the electrodes will influence the transfer of electrons and transport of ions, thus altering the electrode reaction and current response (Morris et al., 1987; Seibold et al., 1989; Mirkin et al., 1990; Chen & Kucernak, 2002). Thus, for nanoscale electrochemical electrodes, it is important to know how the EDL structure affects the electron transfer and current response. When used for biosensing, the electrochemical performances of nanostructured electrodes will also vary with functionalization methods and molecules as well as kinetics of mass transport, in addition to geometrical shapes and dimensions of the nanostructures. These aspects of nanostructure-based electrochemical electrodes are discussed here.

Nanopillar Array Electrodes

Slender nanostructures such as nanowires, nanotubes, and nanorods can now be routinely fabricated using chemical vapor deposition (CVD), physical vapor deposition (PVD), and template-based electrodeposition technique (Lau et al., 2003; Fan et al., 2004; Anandan et al., 2005, 2006). But not all these slender nanostructures are suitable for electrochemical applications. For example, vertically standing carbon nanotubes and silicon nanorods developed by CVD and PVD are not able to sustain the capillary forces generated by the nanostructure–liquid interaction (Lau et al., 2003; Fan et al., 2004). As shown in Figure 6.1A, standing silicon nanorod arrays fabricated by PVD technique deformed severely upon water contact due to the aqueous capillary interaction between the nanostructures and the liquid medium (Kralchevsky & Nagayama, 2000; Fan et al., 2004) as well as the amorphous nature of the silicone nanostructures.

This kind of deformation in the nanostructures upon liquid interaction poses a serious problem for their application in electrochemical biosensors. Although a much improved situation is achieved by annealing silver

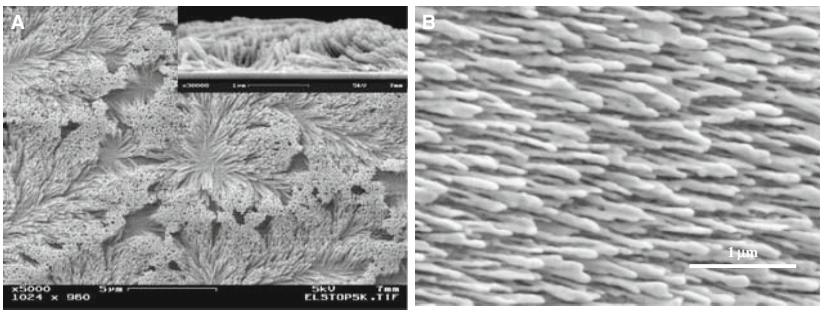

Figure 6.1 Nanorod arrays fabricated by a PVD technique: (**A**) silicon nanorods and (**B**) silver nanorods.

nanorods prior to electrochemical evaluations (see Figure 6.1B; Tang et al., 2006), a better alternative is to use nanostructures fabricated by a cost-effective aqueous-based electrodeposition technique (Anandan et al., 2005; Rao et al., 2005).

This electrodeposition technique takes a three-step fabrication process: (1) fabricating porous anodic alumina (PAA) templates by anodization, (2) depositing nanopillar arrays using the PAA templates, (3) removing the PAA templates. Some representative SEM images of PAA templates developed by the anodization technique are shown in Figure 6.2A (a top view) and Figure 6.2B (a side view), and SEM images of the electrodeposited nanopillar array structures are shown in Figure 6.2C (silver) and Figure 6.2D (gold).

In addition to producing strong vertically aligned nanopillar array structures, this electrodeposition method allows a control of the nanopillar diameter and spacing by simply adjusting the anodization potential (Figure 6.3A) based on the relationships of PD (nm) = 1.35 (nm/V) × AP (V) and PS (nm) = 2.58 (nm/V) × AP (V), where PD stands for the nanopillar diameter, PS the nanopillar spacing, and AP the anodization potential (Rao et al., 2005). When these nanopillar array structures are used as electrochemical electrodes, their active area will increase significantly, which in turn will lead to enhanced current responses. Figure 6.3B shows a series of cyclic voltammograms of a gold nanopillar array electrode in 0.3 M sulfuric acid solution where it is seen that both the oxidation and reduction current responses increase as the height (or the roughness factor) of the nanopillars increases.

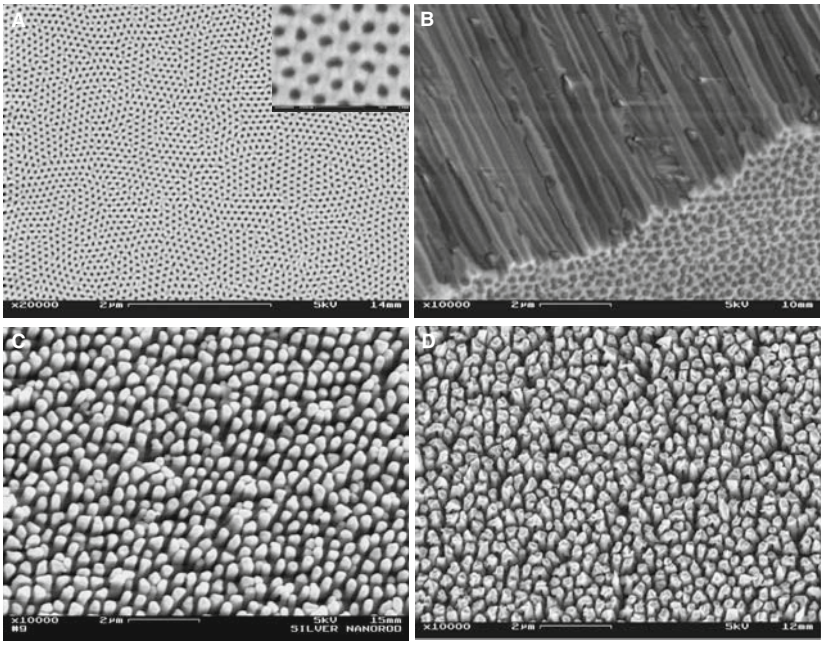

Figure 6.2 Scanning electron microscopic views of PAA templates and electrodeposited nanopillar array structures: (**A**) a top view of a PAA template, (**B**) a side view of a PAA template, (**C**) electrodeposited silver nanopillar array structures, and (**D**) electrodeposited gold nanopillar array structures.

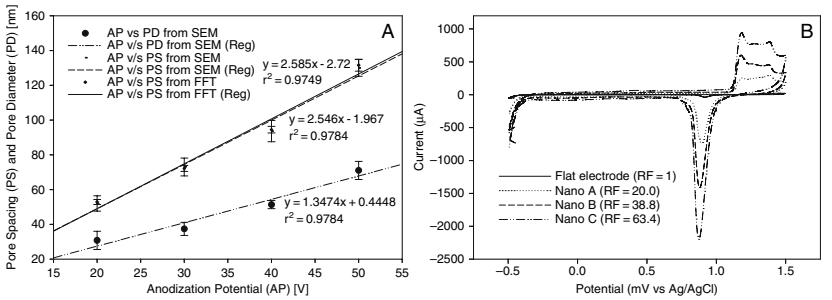

Figure 6.3 (**A**) Calibration curves for the anodization potential (AP) dependent pore spacing (PS) and pore diameter (PD). (**B**) Voltammograms of electrodes made of gold nanopillar array structures with different nanopillar heights and a flat surface (note that RF stands for the roughness factor determined by the ratio of the area under the reduction peak between a nanostructured surface and a flat surface).

Amperometric and Voltammetric Responses of Nanopillar Array Electrodes

With nanopillar array electrodes, much-enhanced electrical currents in both amperometric and voltammetric processes are observed. Figure 6.4A shows the amperometric current responses of bare (non-functionalized) nanopillar array electrodes at various concentrations of $K_4Fe(CN)_6$ under a constant potential of 350 mV (versus Ag/AgCl) in 0.5 M Na_2SO_4 solution. Figure 6.4B shows the amperometric current responses of functionalized

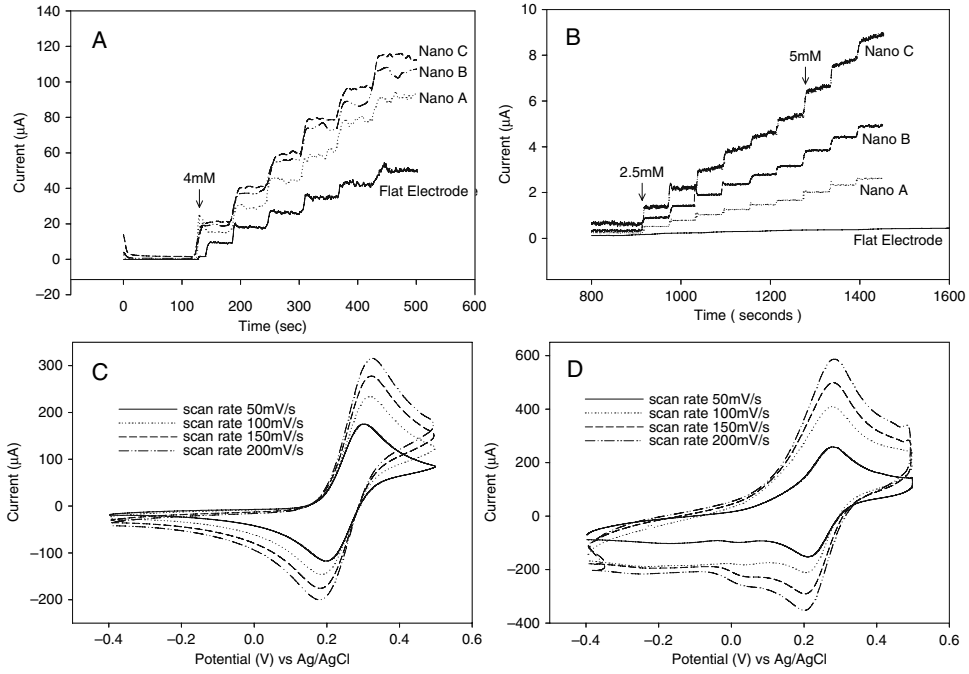

Figure 6.4 (**A**) Amperometric current responses of bare nanopillar array electrodes at various concentrations of $K_4Fe(CN)_6$. (**B**) Amperometric current responses of functionalized nanopillar array electrodes at different glucose concentrations. (**C**) Voltammetric current responses of a flat electrode at various sweep rates. (**D**) Voltammetric current responses of a nanopillar array electrode at various sweep rates.

(with glucose oxidase) nanopillar array electrodes at different glucose concentrations. In general, the nanopillar array electrodes exhibit higher currents than the flat electrode in bare condition for oxidizing $K_4Fe(CN)_6$ and in functionalized condition for oxidizing glucose.

Figure 6.4C and D shows the voltammetric current responses of a flat electrode and a nanopillar array electrode at various sweep rates (50 mV/s, 100 mV/s, 150 mV/s, and 200 mV/s) in a potential range of –0.4 V to +0.5 V against Ag/AgCl in 0.5 M Na_2SO_4 and 4 mM $K_4[Fe(CN)_6]$ (note that the electrodes have the same geometric area, about 16 mm^2). The redox peaks for the $[Fe(CN)_6]^{4-}/[Fe(CN)_6]^{3-}$ couple are higher for the nanopillar array electrodes (Figure 6.4D) than for the flat electrode (Figure 6.4C), and that the peak current increases with increasing scan rate. The oxidation–reduction peak separation (∇E_p) of the voltammograms for the nanopillar array electrode is measured to be about 70 mV, which is close to an ideal Nernstian behavior ($\nabla E_p = 56.4$ mV) (Bard & Faulkner, 2001). Comparing it with ∇E_p for the flat electrode (~110 mV), it is clear that the mass transport at the nanopillar array electrode is significantly enhanced.

Impedance Measurements of Nanopillar Array Electrodes

In an electrochemical process, the change in electrode impedance can be used to characterize the interfacial properties between the electrode and solution. This feature is often exploited in affinity-based electrochemical biosensors, in which changes in electrode impedance caused by molecular binding are measured (Laureyn et al., 2000; Ma et al., 2006). With an avidin–biotin couple, the change in the impedance of nanopillar array electrodes at various degrees of avidin–biotin binding has been characterized (Lee et al., 2008). To prepare the nanopillar array electrodes, avidin is first immobilized with the use of a self-assembled monolayer (SAM) of 11-mercapto- undecanoic acid (MUA) and the subsequent activation of the COOH-terminated group of MUA. Following that, the impedance of such avidin functionalized electrodes is measured in PBS (0.01 M, pH 7.4) with increasing biotin concentrations (from 1 ng/ml to 50 ng/ml).

To show the advantage or disadvantage of impedance measurements versus voltammetric measurements in detecting avidin–biotin binding, both the impedance and voltammetric responses are measured in PBS having 2.5 mM K_4[Fe(CN)6] and 2.5 mM K_3[Fe(CN)6]. The obtained Nyquist plots and voltammograms at various biotin concentrations are shown in Figure 6.5. From the voltammetric responses (Figure 6.5A), it is seen that the highest current level decreases with the increase of biotin concentration. Furthermore, as the biotin concentration increases, the voltammetric curve becomes less peak shaped and more sigmoid shaped. This can be attributed to the increased electron transfer resistance causing the slowdown of the redox activity such that the rate of diffusion becomes equivalent to the rate of oxidation. At a higher biotin concentration (>8 ng/ml), however, the voltammograms seem to stack on top of each other, making it difficult to distinguish the concentration-dependent current responses.

This is not the case with the impedance measurements. The impedance measurements show that the radius of these semicircular Nyquist plots (Figure 6.5B) increases as the biotin concentration increases (causing more

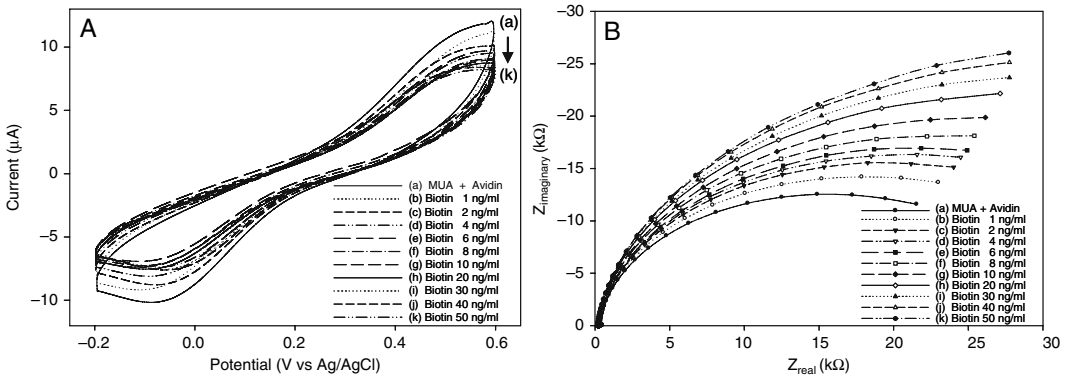

Figure 6.5 Voltammograms (**A**) and Nyquist plots (**B**) obtained for nanopillar array electrodes functionalized with avidin at various biotin concentrations.

biotin to bind to avidin). Therefore, the impedance-based sensing technique with nanopillar array electrodes can provide very good sensitivity and low detection limit (1 ng/ml) with distinct Nyquist plots at different biotin concentrations. By contrast, the voltammetric measurements are less sensitive to the change in biotin concentration, especially at a high concentration of biotin.

Interdigitated Electrodes

For affinity-based biosensing, impedance measurements surely have some advantages. But the drawback is that an impedance-based detection method is very time consuming (Yang et al., 2004): it may take hours to complete a test run during which the electrochemical environment may have changed. In contrast, voltammetric measurements are known for their fast response and ease of use, although they suffer from lack of sufficient sensitivity and lower detection limit. To alleviate this problem, integration of a voltammetric method with interdigitated electrodes (IDEs) has been explored recently (Yang & Zhang, 2005, 2006, 2007).

In IDEs, generator electrodes are placed side by side with collector electrodes in an interdigitated manner. With IDEs, an electroactive species gets oxidized at the generators, diffuses across the thin-layer gap due to a concentration gradient, and gets reduced at the collectors. The reduced species at the collectors then diffuses back to the generators following its concentration gradient. This redox cycling (or feedback) activity makes the measured currents at both the generators and collectors extremely high. Because of the proximity of the generators and collectors, a very high percentage of the oxidized species produced at the generators gets reduced at the collectors with a very low solution resistance (Aoki, 1990; Niwa et al., 1990; Paeschke et al., 1995; Phillips & Stone, 1997; Jeng, et al., 2001). Additionally, a steady-state current can be achieved at IDEs by holding the collectors at a fixed potential while sweeping the potential at the generators.

It has been shown that that the presence of the generators and collectors in nanometer proximity facilitated feedback cycling of oxidation and reduction with extremely high mass transport efficiency, thus leading to high current response and steady-state sigmoidal voltammogram.

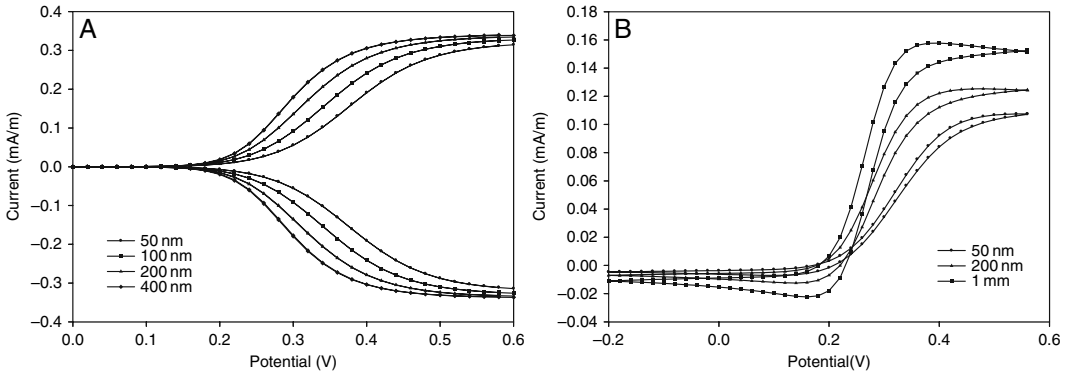

Figure 6.6 (**A**) Sigmoidal voltammograms obtained for IDEs electrodes. (**B**) Peak-shaped voltammograms obtained for single electrodes.

Figure 6.6A shows the voltammograms for IDEs with an electrode width less than 500 nm. Owing to the highly efficient redox cycling, the steady-state current levels at both the anode and cathode are very close despite the significant difference in their electrode widths. By contrast, single electrodes behave quite differently because of a lack of the redox cycling. As shown in Figure 6.6B, the voltammograms obtained for single electrodes are peak shaped with hysteresis, indicating a low efficiency in mass transport by diffusion. Furthermore, the current levels are much lower than those obtained for the IDEs.

When these IDEs are used in biosensors, their current response will rely on the redox cycling behavior and mass transport phenomena at and near the electrode/solution interface which will be altered by the electrode functionalization and further probe/target recognition or binding. Thus, the current response will depend on the electron transfer rate constant (i.e., the k_0 value) of the electrode reactions involved. A decreasing k_0 value represents a situation in which increasing molecular binding may occur at the electrode surface. Figure 6.7 shows the voltammograms at various

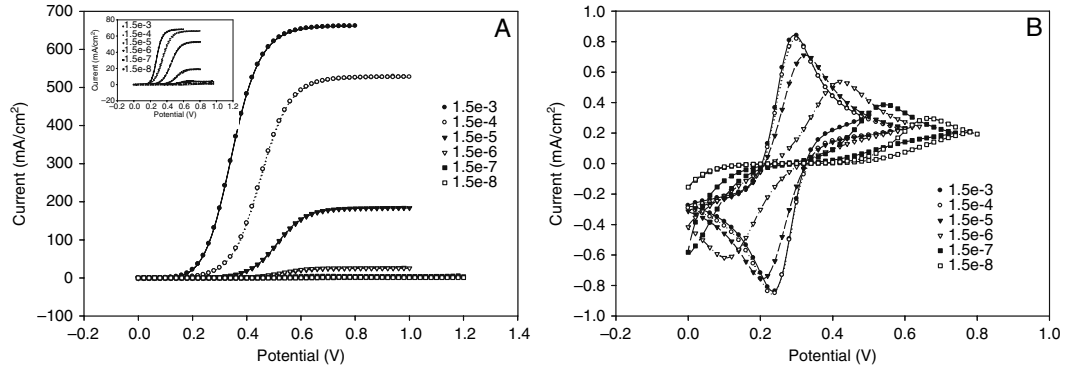

Figure 6.7 Voltammograms obtained for the IDEs with $w = 100$ nm (**A**) and for the single electrode (**B**) at various k_0 values (from 1.5×10^{-3} m/s to 1.5×10^{-9} m/s). The insert shows the voltammograms for the IDEs with $w = 1$ μm.

k_0 values for an IDEs electrode (with a critical dimension of 100 nm; Figure 6.7A) and a single electrode (Figure 6.7B).

For the single electrode, peak-shaped voltammograms are produced when the k_0 value is high. As the k_0 value decreases, the peak current of the voltammogram decreases. This suggests that the rate of diffusion and the rate of oxidation become equivalent, as is the case for the nanopillar array electrodes in avidin–biotin binding experiments (see Figure 6.5A). In comparison, steady-state voltammograms with sigmoidal shape are obtained for the IDEs. At a higher k_0 value, the limiting current obtained for the three IDEs is much higher (hundreds times higher) than the peak current for the single electrode. This increased current response is attributed to the enhanced mass transport near the IDEs. As k_0 decreases, a decrease in the limiting (or peak) current is observed in both cases, but a more drastic decrease is seen with the IDEs than with the single electrode. This fact suggests that the voltammetric performance of IDEs is more sensitive to the change of k_0 as compared with that of the single electrode.

From Figure 6.7A it is seen that the narrower the electrode gets, the more sensitive it becomes to the change of k_0, especially when k_0 is large ($>1.5\times10^{-6}$). For instance, a change in k_0 from 1.5×10^{-3} to 1.5×10^{-4} caused almost a 20% reduction in the limiting current for the IDEs with $w = 100$ nm (Figure 6.7A), whereas a mere 3% reduction was seen for the IDEs with $w = 1$ μm (Figure 6.7A insert). With each set of IDEs, as k_0 decreases, not only the limiting current decreases significantly but also the voltammogram shifts to the right. These facts indicate that the voltammetric current response of the IDEs is indeed sensitive to the change of k_0, and that a higher overpotential is needed to drive the electron transfer as k_0 decreases.

In a more recent study by Strutwolf and Williams (2005) and Yang and Zhang (2007), it is found that the sensing performance can be further enhanced by using 3D IDEs. As shown in Figure 6.8, the limiting current is the highest, intermediate, and the lowest for the nanorod-

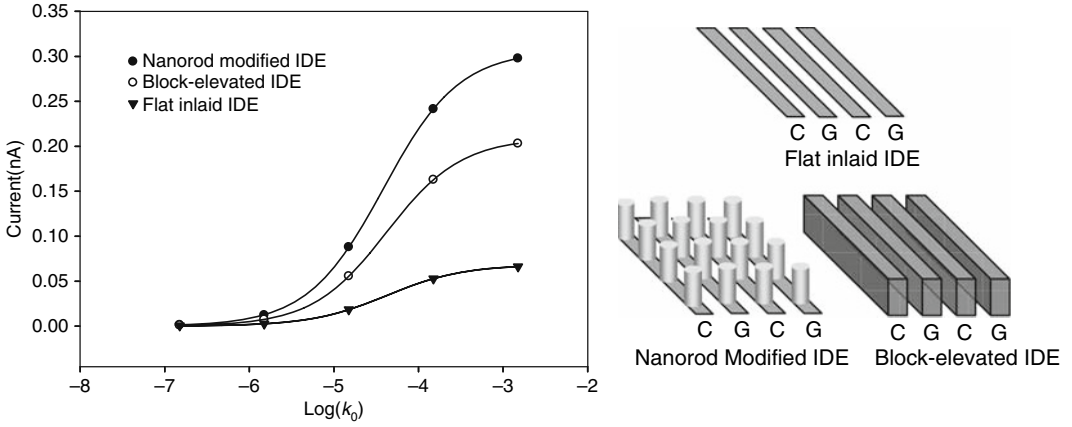

Figure 6.8 Variation of the voltammetric limiting current with $\log(k_0)$ for three 3D IDEs cases: nanorod modified IDE, block-elevated IDE, and flat inlaid IDE. Note that the width for the base collector (C) and generator (G) electrodes is 100 nm in all three cases.

modified, block-elevated, and inlaid IDEs, respectively, at any given k_0. This is attributed to the increased surface area of the electrodes caused by the larger height of the 3D electrodes, which enable a heightened redox cycling activity between the vertical walls of the neighboring generator and collector electrodes.

Effect of Functionalization Molecules and Kinetics of Mass Transport

For nanopillar array electrodes, their electrochemical-based biosensing performances are affected by the type of functionalization molecules used to immobilize the sensitive elements. In the case of self-assembled monolayer (SAM) molecules, their chain length and surface coverage will affect electron transfer. For example, when two SAMs with different chain lengths are used as the underlying molecules for immobilizing glucose oxidase onto the nanopillar array electrodes, they present different electron transfer resistances and detection sensitivities. As shown in Figure 6.9, significantly higher detection sensitivity is achieved for the case with a shorter SAM (i.e., 3-mercaptopropionic acid, or MPA) than for the case with a longer SAM (i.e., 11-mercaptoundecanoic acid, or MUA). This is true for the nanopillar array electrodes with three different nanopillar heights (1 μm, 2 μm, and 3 μm). This result can be attributed to the fact that a shorter SAM is likely to form highly ordered SAM coverage over a larger area and to hold the enzyme at a closer distance to the electrode surface, both of which are crucial for facilitating enhanced electron transfer. Furthermore, in each SAM case, the taller the nanopillars the higher the detection sensitivity. This is due to the increased surface area of the electrodes because of the increased nanopillar height.

The kinetics of mass transport near the electrode/solution interface also plays an important role influencing the current responses of electrochemical-based biosensors (Anandan et al., 2007). When bare nanopillar array electrodes are tested for the redox of $K_4Fe(CN)_6$ at various concentrations, electrodes with different nanopillar heights exhibit almost the same sensitivity response (see Table 6.1), although the sensitivity of nanopillar array

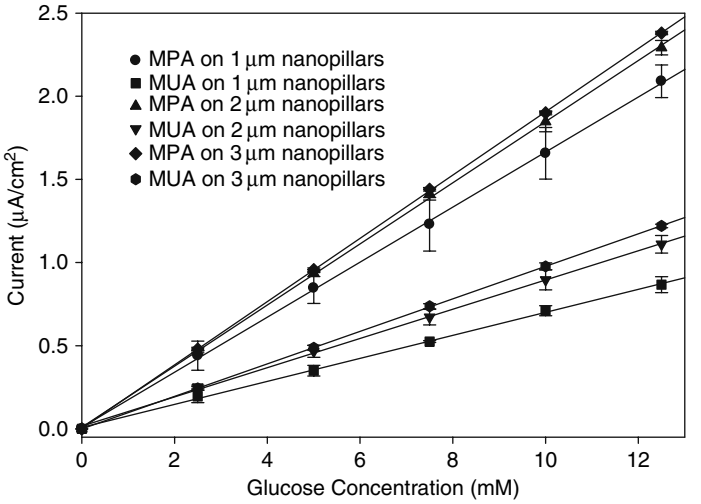

Figure 6.9 Calibration curves of the amperometric steady-state current versus glucose concentration. Cases considered here include nanopillar array electrodes of three different nanopillar heights and two different immobilization molecules.

Table 6.1 Measured values for the roughness ratio, detection sensitivity, and K_m for various nanopillar array electrodes and flat electrode.

Specimen	Roughness factor	Sensitivity of bare electrodes to $K_4Fe(CN)_6$ ($\mu A/mM \cdot cm^2$)	Sensitivity of functionalized electrodes to glucose ($\mu A/mM \cdot cm^2$)	K_m glucose (mM)
Flat	1.0	19.30	0.27	24.8
Nano A	20.0	41.40	0.91	29.3
Nano B	38.8	41.05	1.80	32.6
Nano C	63.4	41.70	3.13	52.0

electrodes is much higher than that of the flat electrode. It is speculated that the electroactive species $K_4Fe(CN)_6$ may encounter certain difficulties in its transport to the small spaces between the nanopillars as a result of either a low diffusivity or a fast-electron transfer rate constant. When the diffusivity is low, it will be difficult for $K_4Fe(CN)_6$ to diffuse deep into the small spaces between the nanopillars, and when the electron transfer rate constant is high, most of the species $K_4Fe(CN)_6$ will get oxidized near the top ends of the nanopillars before it gets diffused deep down the gaps. Under these circumstances, it is conceivable that only the top ends of the nanopillars are serving their active duty in transferring electrons to oxidize $K_4Fe(CN)_6$. The situation for functionalized nanopillar array electrodes (with glucose oxidase) is quite different. The sensitivity of these nanopillar array electrodes in glucose detection increases as the height of the nanopillars (or the roughness ratio) increases. An increase of about 12 times in sensitivity is observed for a nanostructured electrode having a roughness factor of 63.4 as compared with the flat electrode (see Table 6.1).

An enzymatic kinetics study using the Michaelis–Menten equation indicates that the apparent Michaelis–Menten constant (K_m) increases with the presence of nanopillars and increase of their height. As listed in Table 6.1, the K_m values for the nanostructured electrodes are higher than the intrinsic K_m value (25 mM) for dissolved glucose oxidase (Calvo & Wolosiuk, 2004). This implies that the activity of the enzyme immobilized onto these nanostructured electrodes has actually decreased as compared with the freely dissolved enzyme, suggesting that the increase in sensitivity in the functionalized nanopillar array electrodes is due to factors other than enzyme activity.

That the nanostructure-induced sensitivity enhancement for the functionalized electrodes (11.6 times) is higher than that for the bare electrodes (2 times) may be attributed to the difference in electrochemical reactions and kinetics of transport. But these two electroactive species (i.e., glucose and $K_4Fe(CN)_6$) have a similar value of diffusivity (8×10^{-10} m^2/s for $K_4Fe(CN)_6$ and $7.6\times10^{-10} m^2/s$ for glucose) (Winkler, 1995); it is thus possible that different electrode reactions involved in these two cases may play a more dominate role in affecting the current responses. This speculation is confirmed by a computer simulation of the situation.

Figure 6.10A shows the simulated amperometric current responses obtained for a functionalized nanopillar electrode and a flat electrode with the surface-reaction rate constants set at 5×10^{-4} m/s, 5×10^{-5} m/s,

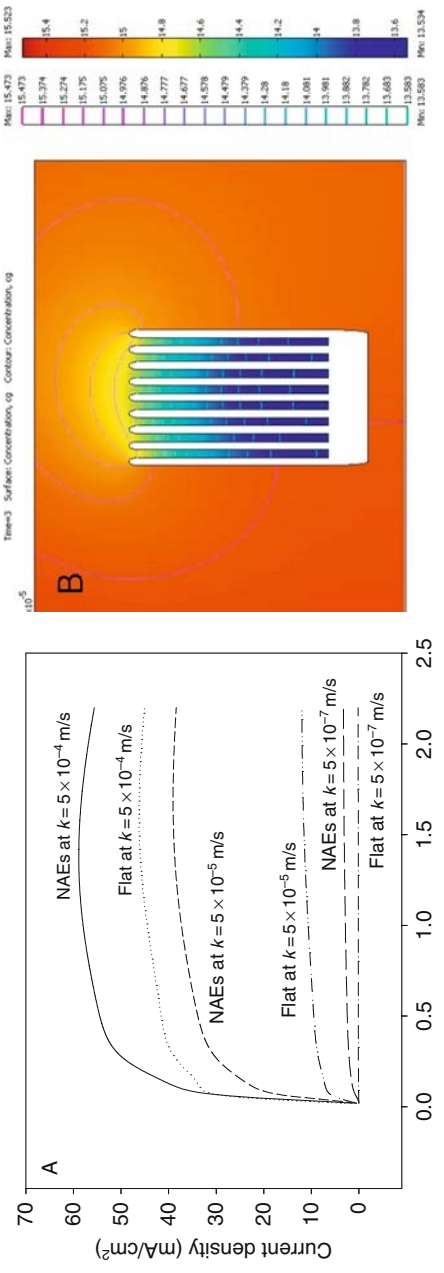

Figure 6.10 (**A**) Simulated current response for a functionalized nanopillar electrode and a flat electrode at various surface-reaction rate constants. (**B**) Contour plot of glucose concentration near the nanopillar electrode obtained at a reaction rate constant of 5×10^{-7} m/s. (*See* Color Plate 12)

Table 6.2 Simulated steady-state amperometric current obtained at various reaction rate constants.

	Current density (mA/cm^2)		
Reaction rate constant (m/s)	**Nano**	**Flat**	**Nano/flat**
5×10^{-4}	58.9	46.2	1.27
5×10^{-5}	39.1	12.0	3.26
5×10^{-7}	3.25	0.146	22.26

and 5×10^{-7} m/s. As expected, a higher current response is seen for the nanostructured electrode than for the flat electrode (see Table 6.2). But the increase in the current response due to the presence of nanopillars is significantly affected by the surface-reaction rate constant for glucose. At a rate constant of 5×10^{-4} m/s, the increase in current due to nanopillars is 1.27-fold, whereas at a rate constant of 5×10^{-7} m/s the increase is 22.26-fold (see Table 6.2).

At a higher surface-reaction rate constant, glucose gets easily oxidized at the top ends of the nanopillars before it can diffuse deep into the space between the nanopillars, while at a lower rate constant, more glucose will be able to diffuse into the deep space between the nanopillars to get oxidized, thus leading to a higher enhanced current response as compared with a flat electrode. These arguments are supported by the fact that a higher glucose concentration is found at the bottom of the spaces between nanopillars in the case with a lower reaction rate constant. The glucose concentration is found to be 0.285 mol/m^3, 0.497 mol/m^3, and 13.583 mol/m^3, respectively, at the bottom of the spaces between nanopillars for cases with the rate constant of 5×10^{-4} m/s, 5×10^{-5} m/s, and 5×10^{-7} m/s. Figure 6.10B shows a contour plot for glucose concentration at a rate constant of 5×10^{-7} m/s, where it is seen that a significant amount of glucose reached to the bottom of the spaces between nanopillars.

These results indicate that the enhanced current response in glucose sensing with functionalized nanostructured electrodes can be attributed to the effective mass transport facilitated by the relatively low reaction rate constant of glucose. Since in most experiments the reaction rate constant cannot be altered easily, it is thus necessary to optimize the dimensions and geometries of the nanopillars (in terms of their diameter, spacing, and height, etc.) in order to accommodate the specific analyte species for achieving the highest possible efficiency in mass transport and electron transfer.

Effect of Electrical Double Layer

The electrical double layer (EDL) structure surrounding the nanometer-scale electrodes will affect their electron transfer and current response (Martynov & Salem 1983; He at al., 2006; Yang & Zhang, 2007). Figure 6.11A shows the voltammograms (normalized to their corresponding limiting current obtained when the effect of EDL is not considered) for electrodes of various sizes when the charge valence (z) of the redox species

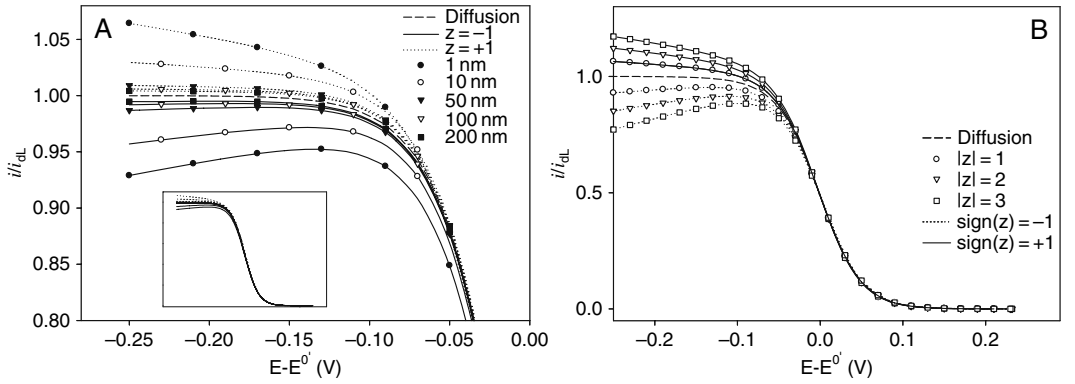

Figure 6.11 (**A**) The reduction end of the simulated voltammograms for single nanometer electrodes of various sizes (from 1 nm to 200 nm). The insert shows the entire voltammograms. (**B**) Simulated voltammograms for an electrode of $r_0 = 1$ nm when the reactant species has different charge valences.

is $z = \pm 1$. Clearly, all the voltammograms exhibit a sigmoidal shape and the curves with $z = 1$ have their normalized limiting current higher than unity while the curves with $z = -1$ have the normalized limiting current lower than unity. This is so because at a negative (reduction) electrode potential the positive-charged redox species would experience attraction and the negative-charged species repulsion, thus causing the current to be either enhanced or suppressed in the respective conditions. In view of the limiting current, the smaller the electrode becomes, the more the normalized limiting current deviates from unity. This EDL-induced current change becomes negligible when the size of the electrode is sufficiently large (>100 nm). In addition to the size effect, the charge valence of the redox species also affects the current response: the higher the charge valence (in its absolute value) is, the more the normalized current deviates from unity (see Figure 6.11B).

Future Perspective

The integration of nanotechnology and biotechnology holds great promises for the realization of autonomous systems for advanced diagnostics and therapies. These systems will perform both biosensing and drug delivery functions. They will make it possible to constantly monitor the biological conditions, process the information in real time, and administer the drug at a desired location, rate, and amount when necessary. These devices can be either micro- or nano-electromechanical systems equipped with biosensors, on-board drugs, and a computer or entirely organic molecular assemblies (e.g., molecular machines) conjugated with specific drug moieties as well as target and environmental-sensitive moieties for site recognition, cell-wall penetration, and drug releasing. These systems will bring benefits of reduced intrusiveness, increased patient comfort, greater fidelity of sensing results, and greater precision for site, amount, and rate controllable drug delivery.

In the coming years, it is anticipated that nanotechnology-based biosensors will continue to evolve and expand their use in many areas of life

sciences, particularly in biomedical diagnosis and drug delivery. For drug delivery applications, these biosensors are expected to possess some ideal features such as high sensitivity, high specificity, fast response and action, low detection limit (such that an early detection of clinically significant proteins and cancer markers is possible), continuous and long-term monitoring capability, carrier of personalized medicine for site-specific and rate-controlled delivery, passively operational (carries no battery, or turns the physiological metabolic events into fuel power), and wirelessly operational (be able to communicate with external monitoring devices wirelessly).

Acknowledgment. Many thanks to my students Y.L. Rao, V. Anandan, X. Yang, R. Cai, X. Tang and postdoctoral fellow S.J. Lee for their contributions to the work discussed here. The financial supports from the National Science Foundation, the University of Georgia Research Foundation, the Faculty of Engineering and the College of Agricultural and Environmental Science at The University of Georgia are acknowledged.

References

Aboubakar, M., Couvreur, P., Pinto-Alphandary, H. & Couritin, B. (2000). Drug Dev Res, 49, 109–117.

Alivisatos P. (2004). The use of nanocrystals in biological detection, Nature Technology, 22, 1, 47–52.

Anandan, A., Rao, Y. L. & Zhang, G. (2005). Nanopillar arrays with superior mechanical strength and optimal spacing for high sensitivity biosensors. Proceedings of Nanotech, 217–220.

Anandan, V., Rao, Y. L. & Zhang, G. (2006). Nanopillar Array Structures for Enhancing Biosensing Performance, Int J Nanomedicine 1(1), 73–79.

Anandan, V., Yang, X., Kim, E., Rao, Y.L. & Zhang, G. (2007). Role of reaction kinetics and mass transport in glucose sensing with nanopillar array electrodes, Journal of Biological Engineering, 1–5.

Aoki, K. (1990). Approximate Models of Interdigitated Array Electrodes for Evaluating Steady-State Currents. J Electroanal Chem, 284, 35–42.

Arrigan, D. W. M. (2004). Nanoelectrodes, nanoelectrode arrays and their applications, Analyst, 129, 1157–1165.

Bard, A. & Faulkner, L. (2001). Electrochemical Methods: Fundamentals and Applications, 2nd Edition, New York: John Wiley and Sons.

Barratt, G., Courraze, G., Couvreur, P. & Dubernet, C. (2002). Polymeric Materials, (Dumitriu, S., Ed). Dekker, New York, 753–782.

Bashir, R. (2004). BioMEMS: state-of-the-art in detection, opportunities and prospects, Adv Drug Deliv Rev 56, 1–22.

Berger, R., Delamarche, E., Lang, H. P., Gerber, C., Gimzewski, J. K., Meyer, E. & Guntherodt, H. J. (1997). Surface stress in the self-assembly of alkanethiols on gold, Science 276, 2021–2023.

Besteman, K., Lee, J. L., Wiertz, F. G. M., Heering, H. A. & Dekker, C. (2003). Nano Lett 3, 727.

Bharathi, S. & Nogami, M. (2001). A glucose biosensor based on electrodeposited biocomposites of gold nanoparticles and glucose oxidase enzyme. Analyst 126, 1919–1922.

Borkholder, D. A., Bao, J., Maluf, N. I., Perl., E. R. & Kovacs, G. T. A. (1997). Microelectrode arrays for stimulation of neural slice preparations, J Neurosci Methods 77(1), 61–66.

Bousse, L. (1996). Whole cell biosensors, Sensors and Actuators, B Chem B34, 1–3, 270–275.

Cai, H.L., Lee, H., Hsing, T. M., & Ming, I. (2006). Label-free protein recognition using an aptamer-based impedance measurement assay, Sens. Actuators, B, Chem 114, 433–437.

Calvo, E. J & Wolosiuk, A. (2004). Supramolecular Architectures of Electrostatic Self-Assembled Glucose Oxidase Enzyme Electrodes, Chem Phys Chem 5, 235–239.

Carrion-Vazquez, M., Oberhauser, A. F., Fowler, S. B., Marszalek, P. E., Broedel, S. E., Clarke, J. & Fernandez, M. J. (1999). Mechanical and chemical unfolding of a single protein: A comparison, Biophysics 96, 3694–3699.

Chen, R. J., Bangsaruntip, S. & Dai, H. (2003). Noncovalent functionalization of carbon nanotubes for highly specific electronic biosensors, PANS 100, 4984–4989.

Chen, R. J., Choi, H. C. & Dai, H. (2004) An investigation of the mechanism of electronic sensing of protein adsorption on carbon nanotube devices, JACS 126, 1563–1568.

Chen, S. & Kucernak, A. (2002). The Voltammetric Response of Nanometer-Sized Carbon Electrodes, J Phys Chem B 106, 9396–9404.

Cherian, S., Gupta, R. K., Mullin, B. C. & Thundat, T. (2003). Detection of heavy metal ions using protein-functionalized microcantilever sensors, Biosens Bioelectron 19, 41–46.

Cia, X., Klauke, N., Glidle, A.,Cobbold, P., Smith, G. L. & Cooper J. M. (2002). Ultra-low-volume, real-time measurements of lactate from the single heart cell using Microsystems technology, Anal Chem 74(4), 908–914.

Cui, Y., Wei, Q., Park, H., & Lieber, C. M. (2001). Nanowire nanosensors for highly sensitive and selective detection of biological and chemical species, Science 293, 1289–1292.

Damage, C., Vonderscher, J., Marbach, P. & Pinget, M. (1997). Pharm Res 18, 949–954.

Davis, Z. J., Abadal, G., Kuhn, O., Hansen, O., Grey, F. & Boisen, A. (2002). Fabrication and characterization of nanoresonating devices for mass detection, J Vac Sci Technol B 18(2), 612–616.

Drummond, T. G., Hill, M. G. & Barton, J. K. (2003). Nature Biotechnology 21, 1192–1199.

D'Souza, S. F. (2001). Biosens Bioelectron 16, 337–353.

Emery, S. R., Haskins, W. E. & Nie, S. (1998). J Am Chem Soc 120, 8009.

Fan, J. G., Dyer, D., Zhang, G. & Zhao, Y. P. (2004). Nanocarpet effect: pattern formation during wetting of vertically aligned nanorod arrays. Nanoletters 4, 2133–2138.

Fernandez-Urrusuno, R., Calvo, P, Remunan-Lopez, C. & Vila-Jato, J. L. (1999). Pharm Res 16, 1576–1581.

Ferrari, M. (2005). Cancer nanotechnology: opportunities and challenges, Nat Rev 5, 161–171.

Fritz, J., Cooper, E. B., Gaudet, S., Sorger, P. K., & Manalis, S. R. (2002). Electronic detection of DNA by its intrinsic molecular charge, PNAS 99, 14142–14146.

Gasparac, R., Taft, B.J., Lapierre-Devlin, M.A., Lazareck, A.D., Xu, J.M. & Kelley S.O. (2004). Ultrasensitive electrocatalytic DNA detection at two and three dimensional nanoelectrodes. J Am Chem Soc 126, 12270–12271.

He, R., Chen, S., Yang, F., & Wu, B. (2006). Dynamic Diffuse Double-Layer Model for the Electrochemistry of Nanometer-Sized Electrodes. J Phys Chem B 110, 3262–3270.

Headrick, J. J., Sepaniak, M. J., Lavrik, N. V. & Datskos, P. G. (2003). Enhancing chemi-mechanical transduction in microcantilever chemical sensing by surface modification, Ultramicroscopy 97, 417–424.

Hintsche, R., Moller, B., Dransfeld, I., Wollenberger, U., Scheller, F. & Hoffmann, B. (1991). Chip biosensors on thin-film metal electrodes, Sens Actuators, B Chem B4 (3–4), 287–291.

Hintsche, R., Kruse, Ch., Uhlig, A., Paeschke, M., Lisec, T., Schnakenberg, U. & Wager, B. (1995). Chemical microsensor systems for medical applications in catheters, Sens Actuators, B Chem B27 (1–3), 471–473.

Jeng, P., Yamaguchi, F., Oi, F. & Matsuo, F. (2001). Glucose Sensing Based Interdigitated Array Microelectrode. Anal Sci 17, 841–846.

Knight, C. G. (1981). Liposomes from physical structure to therapeutic applications, Elsevier, Amsterdam.

Koehne, J., Li, J., Cassel, A. M., Chen, H., Ye, Q., Ng, H. T., Han, J. & Meyyappan, M. (2004). The Fabrication and Electrochemical Characterization of Carbon nanotube Nanoelectrode Arrays. J Mater Chem 14, 676–684.

Kralchevsky, P. A. & Nagayama, K. (2000). Capillary interactions between particles bound to interfaces, liquid films and biomembranes. Adv colloid interface sci 85, 145–192.

Krug, J. T., Wang, G. D., Emory, S. R. & Nie, S. (1999), J Am Chem Soc 121, 9208.

Kubik, T., Bogunia-Kubik, K. & Sugisaka, M. (2005). Nanotechnology on duty in medical applications, Curr Pharm Biotechnol 6, 17–33.

Lau, K. K. S., Bico, J. & Teo, K. B. K. (2003). Superhydrophobic carbon nanotube forests. Nanoletters 3, 1701–1705.

Laureyn, W., Nelis, D., Gerwen, P., Baert, K., Hermans, L., Magnée, R., Pireaux, J., & Maes, G. (2000). Nanoscaled interdigitated titanium electrodes for impedimetric biosensing, Sens. Actuator, B, chem 68, 360–370.

Lee, S. J., Anandan, V. & Zhang, G. (2008). Electrochemical fabrication and evaluation of highly sensitive nanorod-modified electrodes for a biotin/avidin system, Biosensors and Bioelectronics, 1117–1124.

Liu, X. & Tan, W. (1999). A fiber-optic evanescent wave DNA biosensor based on novel molecular beacons, Anal Chem 71, 5054–5059.

Ma, K., Zhou, H., & Zoval, Z. (2006). DNA hybridization detection by label free versus impedance amplifying label with impedance spectroscopy, Sens. Actuators, B, Chem 114, 58–64.

Marrazza, G., Chianella, I. & Mascini, M. (1999). Biosens Bioelectron 14, 43–51.

Martynov, G. A. & Salem, R. R. (1983). Electrical double layer at a metal-dilute electrolyte solution interface, New York: Springer-Verlag Berlin Heidelberg.

Mertens, J., Finota, E., Thundat, T., Fabrea, A., Nadal, M. H., Eyraud, V. & Bourillota, E. (2003). Effects of temperature and pressure on microcantilever resonance response, Ultramicro 97, 119–126.

Mirkin, R. B., Fan, F. R. F. & Bard, A. J. (1990). Evaluation of the Tip Shapes of Nanometer Size Microelectrodes, J Electroanal Chem 328, 47–62.

Moerner, W. E. & Orrit, M. (1999). Illuminating single molecules in condensed matter, Science 283, 1670–1676.

Morris, R. B., Franta, D. J. & White, H. S. (1987). Electrochemistry at Pt Electrodes of Width Approaching Molecular Dimensions. Breakdown of Transport Equations at Very Small Electrodes, J Phys Chem 91, 3559–3564.

Moskovits, M. (2005). Surface-enhanced raman spectroscopy: a brief retrospective, J Raman Spectroscopy 36, 485–496.

Nie, S. & Zare, R. N. (1997). Optical detection of single molecules, Ann Rev Biophys Biomol Struct 26, 567–596.

Niwa, O., Morita, M. & Tabei, H. (1990). Electrochemical Behavior of Reversible Redox Species at Interdigitated Array Electrodes With Different Geometries Consideration of Redox Cycling and Collection Efficiency. Anal Chem 62 (5): 447–452.

Paeschke, M., Wollenberger, U., Kiihler, C., Lisec, T., Schnakenberg, U. & Hintsche, R. (1995). Properties of Interdigital Electrode Arrays With Different Geometries. Analytica Chimica Acta 305, 126–136.

Pancrazio, J. J., Bey, P. P., Cuttino, D. S., Kusel, J. K., Borkholder, D. A., Shaffer, K. M., Kovacs, G. T. A. & Stenger, D. A. (1998). Portable cell-based biosensor system for toxin detection, Sens Actuators, B. Chem 53(3), 179–185.

Phillips, C. & Stone, H. (1997). Theoretical Calculation of Collection Efficiencies for Collector-Generator Microelectrode Systems. J Electroanal Chem 437, 157–165.

Popovich, N. D. & Thorp, H. H. (2002). New Strategies for Electrochemical Nucleic Acid Detection, Interface 11(4), 30–34.

Porter, T. L., Eastman, M. P., Macomber, C., Delinger, W. G., & Zhine, R. (2003). An embedded polymer piezoresistive microcantilever sensor, Ultramicroscopy 97, 365–369.

Powers, M. J., Domansky, K. & Griffith, L. G. (2002). A microfabricated array bioreactor for perfused 3D liver culture, Biotechnol Bioeng 78, 3, 257–269.

Rao, L. R., Anandan, V. & Zhang, G. (2005). FFT Analysis of Pore Pattern in Anodized Alumina Formed at Various Conditions, Journal of Nanoscience and Nanotechnology, Vol. 2, No. 12, 2070–2075.

Rao, L. R. & Zhang, G. (2006). Enhancing the Sensitivity of SAW Sensors with Nanostructures, Current Nanoscience 2(4), 311–318.

Ratner, B. D., Hoffman, A. S., Schoen, F. J. & Lemons, J. E. (2004). Biomaterials Science, 2nd Edition, Academic Press.

Reining-Mack, A., Thielecke, H. & Robitzki, A. A. (2002). Trends Biotechol 20, 56–61.

Rider, T. H., Petrovick, M. S. & Hollis, M. A. (2003). A B-cell based sensor for rapid identification of pathogens, Science 301, 213–215.

Sawant, R. M., Hurly, J. P., Salmaso, S. & Torchilin, V. P. (2006). "Smart" drug delivery systems: double-targeted pH-responsive pharmaceutical nanocarriers, Bioconjugate Chem 17, 943–949.

Seibold, J. D., Scott, E. R. & White, H. S. (1989). Diffusion Transport to Nanoscopic Band Electrodes, J Electroanal Chem 264, 281–289.

Sepaniak, M., Datskos, P., Lavrik, N. & Tipple, C. (2002). Microcantilever Transducers: A New Approach in Sensor Technology, Anal Chem 1, 568A–575A.

Sosnowski, R. G., Tu, E., Butler, W. F., O'Connell, J. P. & Heller, M. J. (1997). Rapid Determination of Single Base Mismatch in DNA Hybrids by Direct Electrical Field Control. PNAS 94, 1119–1123.

Stenger, D. A., Gross, G. W., Keefer, E. W., Shaffer, K. M., Andreadis, J. D., Ma, W. & Pancrazio, J. J. (2001). Detection of physiologically active compounds using cell-based biosensors, Trends Biotech 19(8), 304–309.

Stoney, G. G. (1909). Proc R Soc London, serial A, 82, 172–277.

Strutwolf, J. & Willams, D. (2005). Electrochemical Sensor Design Using Coplanar and Elevated Interdigitated Array Electrodes. A computational Study. Electroanalysis 17 (2): 169–177.

Sun, E. Y., Josephson, L., Kelly, K. A. & Weissleder, R. (2006). Development of nanoparticle libraries for biosensing, Bioconjugate Chem 17, 109–113.

Tang, X. J, Zhang, G. & Zhao, Y. P. (2006). Electrochemical characterization of silver nanorod electrodes prepared by oblique angle deposition, Nanotechnology 17, 4439–4444.

Thielecke, H., Mack, A. & Robizki, A. (2001). Anal Bioanal Chem 369, 23–29.

Thundat, T., Wachter, E. A., Sharp, S.L. & Warmack, R. J. (1995). Appl Phys Let 66, 1695–1697.
Umek, R., Lin, M., Vielmetter, S. W. & Chen, D. H. (2001). Chem Mol Diagn 3, 74–84.
Vo-Dinh, T. & Cullum, B. (2000). Biosensors and biochips: advances in biological and medical diagnostics, J Anal Chem 366, 540–551.
Wang, J. & Mustafa, M. (2004). Carbon nanotube screen-printed electrochemical sensors. Analyst 129, 1–2.
Winkler, K. (1995). The kinetics of electron transfer in Fe (CN)6 4–/3– redox system on platinum standard-size and ultramicroelectrodes, J Electroanal Chem 388, 151–159.
Wickline, S. A. & Lanza, G. M. (2003). Nanotechnology for molecular imaging and target therapy, Circulation 107,1092–1095.
Wu, G. H., Datar, R. H., Hansen, K. M., Thundat, T., Cote, R. J. & Majumdar, A. (2001). Bioassay of prostate-specific antigen (PSA) using microcantilevers, Nat Biotechnol 19, 856–860.
Yang, L., Li, Y., & Erf, G. F. (2004). Interdigitated Array Microelectrode-Based Electrochemical Impedance Immunosensor for Detection of Escherichia coli O157:H7, Anal. Chem 76, 1107–1113.
Yang, X. & Zhang, G. (2005). Diffusion-Controlled Diffusion-Controlled Redox Cycling at Nanoscale Interdigitated Electrodes, Proceedings of the COMSOL Multiphysics Conference, 285–290.
Yang, X. & Zhang, G. (2006) Effect of Electron Transfer Rate on the Electrochemical Process of Interdigitated Electrodes, Proceedings of the COMSOL Conference, 233–238.
Yang, X. & Zhang, G. (2007) The Voltammetric Performance of Interdigitated Electrodes with Different Electron-Transfer-Rate Constants, Sens. Actuators, B 126, 624–631.
Yemini, M., Reches, M. & Rishpon, J. (2005). Novel electrochemical biosensing platform using self assembled peptide nanotube. Nanoletters 5, 183–186.
Zhang, G. & Gilbert, J. L, (2004). A New Method for Real-Time and In-Situ Characterization of the Mechanical and Material Properties of Biological Tissue Constructs, Tissue Engineered Medical Products (TEMPs), ASTM STP 1452, Picciolo and Schutte Eds., 120–133.
Zhang, G. (2005). Evaluating the Viscoelastic Properties of Biological Tissues in a New Way. Journal of Musculoskelet Neuronal Interact 5(1), 85–90.
Zhu, H. & Snyder, M. (2003). Curr Opin Chem Biol 7, 55–63.